

Received:
11 June 2015Revised:
6 November 2015Accepted:
9 December 2015

doi: 10.1259/bjr.20150470

Cite this article as:

Park SY, Kim CK, Park JJ, Park BK. Exponential apparent diffusion coefficient in evaluating prostate cancer at 3 T: preliminary experience. *Br J Radiol* 2016; **89**: 20150470.

FULL PAPER

Exponential apparent diffusion coefficient in evaluating prostate cancer at 3 T: preliminary experience

^{1,2}SUNG Y PARK, MD, ^{1,3}CHAN K KIM, MD, ¹JUNG J PARK, MD and ¹BYUNG K PARK, MD¹Department of Radiology and Center for Imaging Science, Samsung Medical Center, Sungkyunkwan, Seoul, Republic of Korea²Department of Radiology and Research Institute of Radiological Science, Severance Hospital, Yonsei University College of Medicine, Seoul, Republic of Korea³Department of Medical Device Management & Research, SAIHST, Sungkyunkwan University, Seoul, Republic of Korea

Address correspondence to: Dr Chan K Kim

E-mail: chankyokim@skku.edu**Objective:** To investigate the feasibility of exponential apparent diffusion coefficient (eADC) derived from diffusion-weighted imaging (DWI) in evaluating prostate cancers at 3 T.**Methods:** 74 consecutive patients with surgically confirmed single peripheral zone (PZ) prostate cancer $\geq 0.5\text{cm}^3$ who underwent pre-operative DWI at 3 T were retrospectively selected. Based on radiological-pathological correlation, eADC and apparent diffusion coefficient (ADC) ($\times 10^{-3}\text{mm}^2\text{s}^{-1}$) for the cancers and benign PZ were measured by two independent readers. Tumour eADC or ADC was correlated with Gleason score. Receiver operating characteristic curve analysis was performed to differentiate between Gleason score 6 and 7 or higher, by eADC and ADC. Lesion-to-background contrast ratio was compared between eADC and ADC.**Results:** Mean tumour eADC (0.48–0.50) and ADC (0.72–0.75) were significantly different from those ofbenign PZ (eADC, 0.20–0.27; ADC, 1.34–1.66), respectively ($p < 0.001$). A moderate correlation between tumour eADC or ADC and Gleason score was seen. For differentiating between Gleason score 6 and 7 or higher, eADC (0.818–0.883) showed a similar area under the curve with ADC (0.840–0.889) ($p > 0.05$). Lesion-to-background contrast ratio of eADC (Reader 1, 2.43; Reader 2, 2.23) was significantly greater than that of ADC (Reader 1, 2.21; Reader 2, 2.12) ($p < 0.001$).**Conclusion:** The eADC may offer similar diagnostic utility with ADC in the differentiation of the cancer from benign prostate tissue. Moreover, the eADC appears to allow improved tissue contrast.**Advances in knowledge:** The eADC may be a comparable alternative to ADC for evaluating prostate cancer, with removing T_2 shine-through effects from DWI.

INTRODUCTION

Many studies have reported that diffusion-weighted imaging (DWI) is useful in evaluating prostate cancer.^{1–4} Currently, DWI is an essential sequence of minimal prostate MRI protocols in the cancer detection and localization.⁵ The apparent diffusion coefficient (ADC) map generated from DWI data reflects the diffusion state of water molecules at the cellular level. A prostate cancer with high cellularity causing the diffusion restriction typically manifests as a focal area of low ADC value on the ADC map. However, some limitations may exist in detecting low-risk cancers with low Gleason score⁶ or predicting central gland cancers⁷ owing to their similar ADC value with background benign prostatic tissues. The ADC values are inversely associated with Gleason scores in prostate cancer,⁸ which may help the pre-treatment risk stratification.⁹

The exponential apparent diffusion coefficient (eADC) is another DWI parameter calculated by the following

equation: $\text{eADC} = S_b/S_0 = e^{-b \times \text{ADC}}$, where S_b and S_0 were signal intensities of DWI when the diffusion sensitization is present or absent, respectively; b was the maximal b value of DWI sequence; and e was the mathematical constant, the base of the natural logarithm.^{10,11} By calculating the ratio of signal intensities (S_b/S_0), the degree of diffusion restriction is positively associated with eADC value. Therefore, the area of more diffusion restriction such as the prostate cancer may show relative hyperintensity (high eADC value) than the adjacent area of less diffusion restriction (low eADC value) on the eADC map.

To date, only a few studies^{11–13} on the clinical applications of eADC have been reported in central nervous system. A recent study in the genitourinary field reported that the eADC map at 3 T was helpful in differentiating renal lesions.¹⁰ To our knowledge, however, no published studies have shown the utility of eADC in evaluating prostate cancer. The purpose of our study was to

retrospectively investigate the feasibility of eADC in evaluating prostate cancers at 3 T.

METHODS AND MATERIALS

Subjects

Institutional review board of Samsung Medical Center approved this retrospective study and waived the requirement for informed consent. Between October 2012 and March 2013, 179 consecutive patients underwent prostate MRI, followed by radical prostatectomy. Of these, a total of 74 patients (mean age, 66.6 ± 6.9 years; range, 52–80 years) met all the following inclusion criteria: (a) pre-operative prostate DWI at 3 T, including ADC and eADC maps, (b) radical prostatectomy, (c) single peripheral zone (PZ) cancer $\geq 0.5 \text{ cm}^3$ and (d) ≤ 2 months of interval time between MRI and surgery. The remaining 105 patients were excluded owing to the following: (a) $< 0.5 \text{ cm}^3$ of the cancer volume ($n = 57$), (b) > 2 months of interval time between MRI and surgery ($n = 25$), (c) patients with surgically proven multiple cancer foci ($n = 12$), (d) absence of the PZ cancer ($n = 8$) and (e) absence of eADC map ($n = 3$). For the reliable correlation between MRI and pathological findings, patients with only cancer foci $< 0.5 \text{ cm}^3$ or multiple cancers were excluded from our analysis.^{14,15}

MRI technique

All prostate MR images were performed 3–5 weeks after the transrectal ultrasound-guided biopsy and before radical prostatectomy using 3-T MRI (Intera Achieva 3TX; Philips Medical System, Best, Netherlands) equipped with a phased-array coil (CARDIAC SENSE, 6-channel). Both T_2 weighted imaging (T2WI) and DWI were included in prostate MRI. Before MRI, 20 mg of butyl scopolamine (Buscopan®; Boehringer Ingelheim, Ingelheim am Rhein, Germany) was injected intramuscularly to suppress bowel peristalsis.

T_2 weighted turbo spin-echo images were acquired in three orthogonal planes (transverse, sagittal and coronal). T2WI parameters were as follows: repetition time (TR)/echo time (TE), 3300–3500/100 ms; slice thickness, 3 mm; interslice gap, 1 mm; field of view, 20 cm; matrix, 568×341 ; number of signals acquired, 3; sensitivity encoding (SENSE) factor, 2; and acquisition time of each plane, 3 min 45 s.

DWI was obtained in the transverse plane using the single shot echoplanar imaging technique (TR/TE, 5250/68–70 ms; slice thickness, 3 mm; interslice gap, 1 mm; matrix, 124×121 ; field of view, 20 cm; SENSE factor, 2; number of signals acquired, 4; b -values, 0, 100 and 1000 s mm^{-2} and acquisition time, 3 min 35 s). The phase-encoding gradient moved from left to right to minimize motion artefacts. According to the equation of $\text{eADC} = S_b/S_0 = e^{-b \times \text{ADC}}$, both ADC and eADC maps were generated. After data acquisition, all images were transferred to the workstation with manufacturer-supplied software (ViewForum Workstation R5.1, Philips Healthcare) for the image analysis.

Histopathological and MRI analyses

All surgical specimens were fixed overnight in 10% buffered formalin. From prostatic base to apex, the transverse sections with an interval of 3 mm were obtained, perpendicular to the

prostatic urethra. An experienced genitourinary pathologist blinded to the MRI findings reviewed all slides of the transverse section, and the cancers were thus localized. The tumour volume, location and Gleason score were also assessed. Under the assumption that the shape of cancer is ellipsoid, the cancer volume was estimated by using the standard ellipsoid formula: $(\text{width} \times \text{height} \times \text{length}) \times \pi/6$, where the width, height and length were measured by a pathologist.

Typical MR findings of PZ cancer were defined as follows: (a) a focal lesion showing low signal intensity on T2WI, compared to the high signal intensity background of benign PZ tissues, and (b) a focally low signal lesion on ADC maps with high signal intensity at $b = 1000 \text{ s mm}^{-2}$ of DWI in comparison with the surrounding benign PZ tissue.⁵ PZ cancers were localized in 6 regions that consisted of right and left side at each base, mid and apex for the radiological–pathological correlation.

Based on the radiological–pathological correlation, two independent radiologists (CKK and SYB, with 8 years and 2 years of experience in prostate MR, respectively) measured both ADC and eADC values in the cancers and benign PZs. For measuring each ADC and eADC value of PZ cancers, an ellipsoid region of interest was first drawn within a cancerous area of ADC map, which was subsequently copied onto the eADC map at the same transverse plane. The same process was applied for measuring both ADC and eADC values in the benign PZ tissues outside the cancerous lesions.

The conventional signal-to-noise ratio and contrast-to-noise ratio were not estimated for both ADC and eADC maps in our study. The background air noise should be measured in the region where respiratory or motion-related artefacts are absent as an integrant of the formula for estimating the signal-to-noise ratio or contrast-to-noise ratio.¹⁶ However, in the background air surrounding the pelvis, measurable noise was seldom found on ADC or eADC maps except for a few motion-related artefacts. Therefore, we calculated the lesion-to-background contrast ratio of ADC and eADC for estimating tissue contrast:¹⁷ the lesion and background were PZ cancer and benign PZ tissue, respectively.

Statistical analysis

All quantitative data were expressed as mean \pm standard deviation. Comparison of ADC or eADC values between PZ cancers and benign PZ tissues was using Student's paired t -test. Correlation between tumour ADC or eADC values and Gleason scores was performed using the Spearman correlation analysis: correlation $\rho < 0.40$, weak correlation; $0.40 \leq$ correlation $\rho \leq 0.75$, moderate correlation; correlation $\rho > 0.75$, excellent correlation.

Tumour ADC or eADC values were compared according to Gleason scores by analysis of variance. Receiver operating characteristic curve analysis was used for differentiating Gleason score 6 from 7 or higher.

The interreader variability was evaluated using the Bland–Altman test. The Wilcoxon signed-rank test was used to

Table 1. Patient characteristics

Variable	Value
Age (years)	66.6 ± 6.9 (52–80)
PSA (ng ml ⁻¹)	11.8 ± 11.7 (1.3–90.9)
Tumour volume (cm ³)	4.1 ± 4.2 (0.5–24.1)
Pathological stage (n)	
2a	7
2b	0
2c	24
3a	29
3b	14
Gleason score (n)	
6	7
7	47
8	7
9	13

PSA, prostate-specific antigen.

Data are the mean values ± standard deviation (range).

compare the lesion-to-background contrast ratio between ADC and eADC maps.

Statistical analysis was performed using SPSS® v. 20.0 (IBM Corp., New York, NY; formerly SPSS Inc., Chicago, IL) and MedCalc v. 12.3.0 (MedCalc Software, Mariakerke, Belgium). A two-sided *p*-value <0.05 was considered statistically significant.

RESULTS

The mean volume of the PZ cancers was 4.1 ± 4.2 cm³. The mean PSA level was 11.8 ± 11.7 ng ml⁻¹. The patient characteristics are summarized in Table 1.

Cancer vs benign tissue

Tumour ADC values were significantly lower than those of benign PZ tissues, while tumour eADC values were significantly

higher than those of benign PZ tissues in both readers (*p* < 0.001) (Table 2) (Figure 1).

Gleason score of cancer

The mean ADC and eADC values of PZ cancers were significantly different among each Gleason score in both readers (*p* < 0.001): all pairwise comparisons of ADC or eADC values were significantly different in both readers (*p* < 0.01), except a comparison between Gleason score 8 and 9 (ADC and eADC of Reader 1, *p* = 0.929 and 0.911, respectively; those of Reader 2, *p* = 0.674 and 0.813, respectively) (Table 3).

Both tumour ADC and eADC values revealed a moderate correlation with Gleason scores: Spearman correlation coefficients of ADC and eADC in Reader 1 were -0.633 and 0.633, respectively, while those in Reader 2 were -0.528 and 0.503, respectively (Figure 2).

For differentiating between Gleason score 6 and 7 or higher, the area under the curves (AUCs) of ADC and eADC were 0.889 (95% confidence interval, 0.795–0.950) and 0.883 (95% confidence interval, 0.787–0.946), respectively, in Reader 1 and were 0.840 (0.736–0.915) and 0.818 (0.711–0.898), respectively, in Reader 2. In the comparison of AUCs between ADC and eADC, no significant difference was seen in Reader 1 (*p* = 0.207) and Reader 2 (*p* = 0.795). In Reader 1, the sensitivity and specificity using the cut-off value of ADC (0.84 × 10⁻³ mm² s⁻¹) vs eADC (0.43) were 82.1% and 85.7% vs 81.0% and 86.0%, respectively; in Reader 2, the sensitivity and specificity using the cut-off value of ADC (0.80 × 10⁻³ mm² s⁻¹) vs eADC (0.45) were 79.1% and 85.2% vs 78.0% and 86.0%, respectively.

Interreader variability

For the interreader variability, a mean difference for the PZ cancers was 5.8% in ADC and 4.0% in eADC, respectively, while that for the benign PZ tissues was 6.0% in ADC and 7.9% in eADC, respectively.

Lesion-to-background contrast ratio

The mean lesion-to-background contrast ratio of eADC was significantly greater than that of ADC in both readers, respectively [Reader 1, 2.21 (1.40–4.16) in ADC vs 2.43

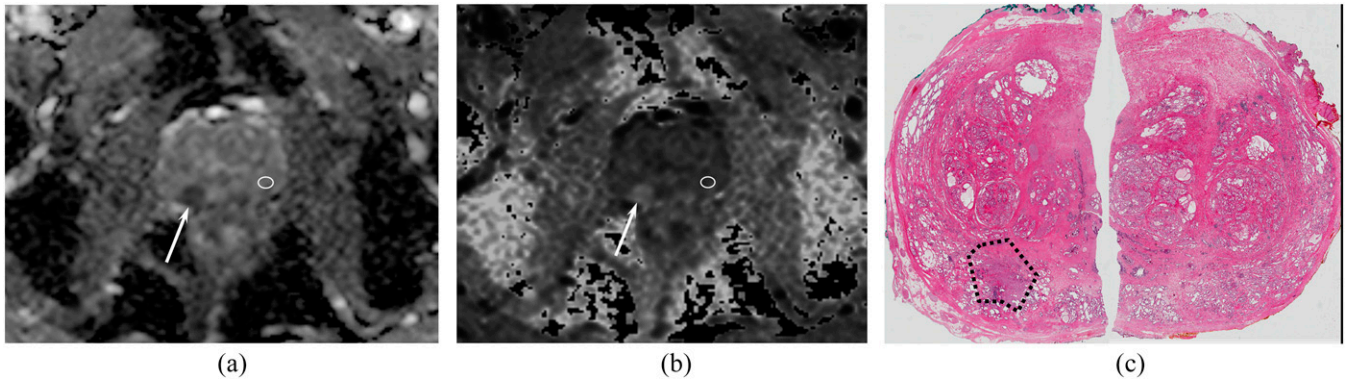
Table 2. Apparent diffusion coefficient (ADC) and exponential apparent diffusion coefficient (eADC) values of peripheral zone (PZ) cancers and benign peripheral zone tissues in the prostate

Variable	PZ cancer	Benign PZ	<i>p</i> -value ^a
Reader 1			
ADC (×10 ⁻³ mm ² s ⁻¹)	0.75 (0.44–1.18)	1.66 (1.22–2.18)	<0.001
eADC	0.48 (0.31–0.64)	0.20 (0.11–0.33)	<0.001
Reader 2			
ADC (×10 ⁻³ mm ² s ⁻¹)	0.72 (0.45–0.98)	1.34 (1.04–1.86)	<0.001
eADC	0.50 (0.38–0.64)	0.27 (0.16–0.36)	<0.001

Data are the mean values (range).

^aStatistical comparison between PZ cancer and benign PZ.

Figure 1. A 61-year-old man with a right peripheral zone (PZ) cancer and Gleason score 7 at surgical specimen. Transverse apparent diffusion coefficient (ADC) (a) and exponential apparent diffusion coefficient (eADC) (b) maps show a focal area (arrows) of low ADC ($0.74 \times 10^{-3} \text{ mm}^2 \text{ s}^{-1}$) and high eADC (0.48) in the right PZ. In the contralateral benign PZ (white regions of interest), both ADC and eADC were $1.31 \times 10^{-3} \text{ mm}^2 \text{ s}^{-1}$ and 0.27, respectively. On the surgical specimen (c), an adenocarcinoma with Gleason score 7 was identified in right PZ (black dotted area).



(1.44–4.12) in eADC; Reader 2, 2.12 (1.47–4.59) in ADC vs 2.23 (1.46–5.64) in eADC; $p < 0.001$] (Table 4).

DISCUSSION

Theoretically, it may be expected that the eADC maps in the prostate cancers have similar characteristics with the ADC maps, since the calculation of eADC ($eADC = S_b/S_0$) is closely related to that of ADC ($ADC = -\ln(S_b/S_0)/b$).¹⁰ Our results demonstrated that the eADC values in the PZ cancers, as ADC values, were significantly different than benign PZ tissues and showed a moderately positive relationship with the Gleason score. Furthermore, eADC revealed greater lesion-to-background contrast ratio than ADC. Therefore, these findings indicate that the eADC might show comparable feasibility with the ADC in evaluating PZ cancers.

Active surveillance of prostate cancer is an important option for the management of low-risk prostate cancers.¹⁸ Aggressiveness of prostate cancer is primarily evaluated by the Gleason grading system. Several studies have reported that the ADC values derived from DWI data were correlated with Gleason scores of prostate cancers located in the PZ,^{8,19} which may aid the pre-treatment risk stratification. Accordingly, DWI may be considered to have a promising role in terms of selecting low-risk prostate cancers, since the Gleason score of ≤ 6 is one of the criteria for determining low-risk cancer.²⁰ In our study, the eADC values in the PZ cancers, similar to the ADC values, were significantly different among each Gleason score, except

a comparison between Gleason score 8 and 9. Both eADC and ADC values had a moderate relationship with the Gleason score. These results were in line with the previous studies.^{8,19} Moreover, receiver operating characteristic curve analysis demonstrated the AUCs of eADC were 0.818–0.883 in differentiating between Gleason score 6 and 7 or higher, which were similar to those of ADC (0.840–0.889). Based on these findings, we believe that the eADC values in the PZ cancers, as the ADC values, may potentially be used as an imaging biomarker to predict the Gleason score.

On the ADC maps, the contrast difference of tissues may be attenuated in comparison with that of eADC maps because the ADC maps are based on the logarithm of S_b/S_0 while the eADC maps are based only on the ratio S_b/S_0 . These may result in reduced lesion-to-background contrast ratio on the ADC maps compared with the eADC maps.¹¹ In our study, the ratio of eADC between PZ cancers and benign PZ tissues was significantly greater than that of ADC. On the basis of our results, the eADC maps may improve the detectability of the PZ cancers without significant loss of the predictability for tumour grade, as compared with the ADC maps. However, a qualitative analysis was not performed in our study. Further studies in a larger population are needed to confirm these findings.

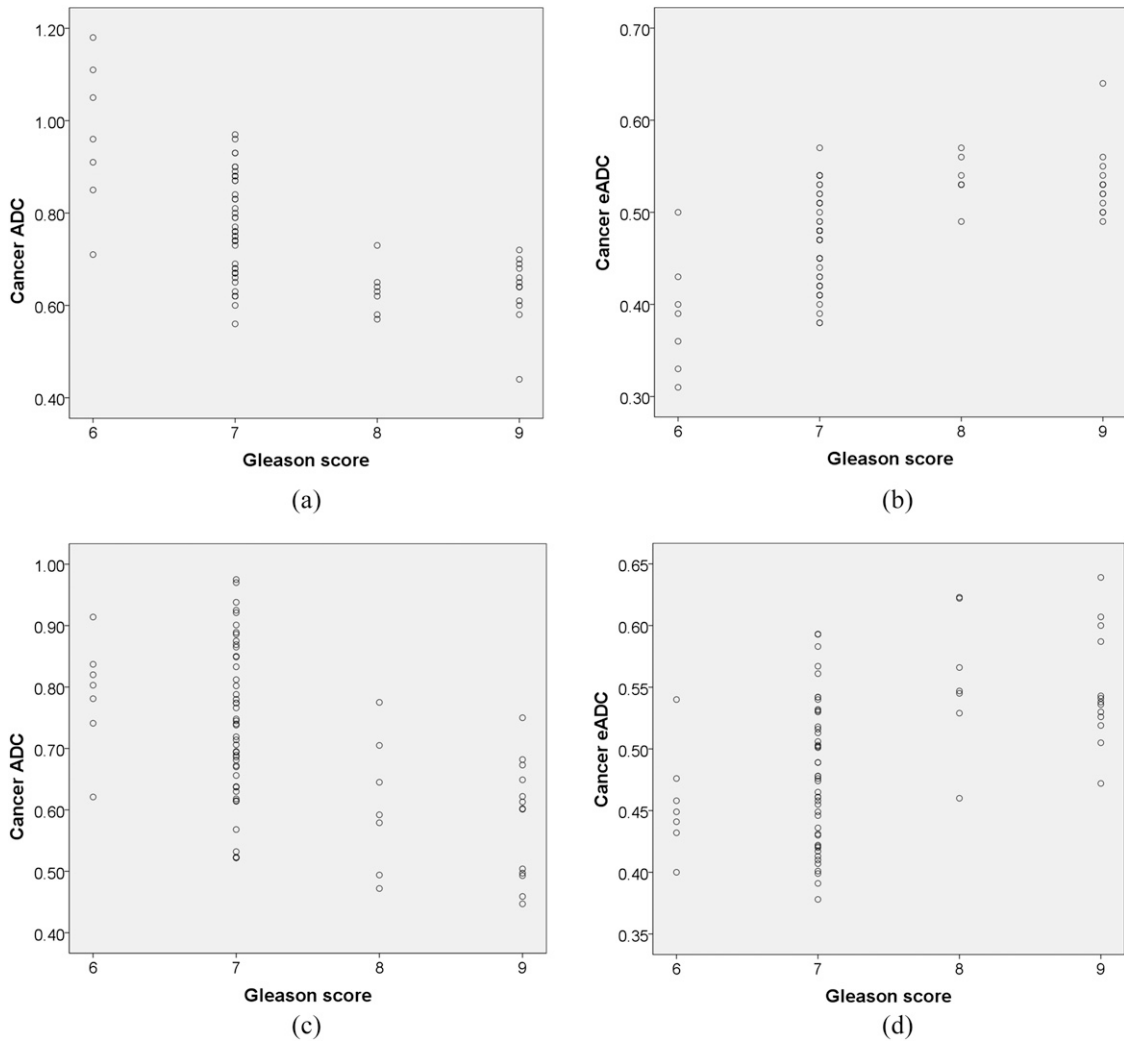
One major prerequisite for the use of eADC as a valuable quantitative method is the reproducibility of measured values. In

Table 3. Apparent diffusion coefficient (ADC) and exponential apparent diffusion coefficient (eADC) values of peripheral zone cancer according to Gleason scores of cancers

Gleason score	Reader 1		Reader 2	
	ADC ($\times 10^{-3} \text{ mm}^2 \text{ s}^{-1}$)	eADC	ADC ($\times 10^{-3} \text{ mm}^2 \text{ s}^{-1}$)	eADC
6	0.97 ± 0.16	0.39 ± 0.06	0.93 ± 0.20	0.40 ± 0.08
7	0.77 ± 0.10	0.47 ± 0.05	0.74 ± 0.12	0.48 ± 0.06
8	0.63 ± 0.05	0.53 ± 0.04	0.61 ± 0.11	0.56 ± 0.06
9	0.64 ± 0.07	0.53 ± 0.06	0.58 ± 0.10	0.55 ± 0.05

Data are the mean values \pm standard deviation (range).

Figure 2. The relationship between apparent diffusion coefficient (ADC) or exponential apparent diffusion coefficient (eADC) and Gleason score of peripheral zone cancers. The cancer dots showing identical ADC or eADC at the same Gleason score totally overlap each other in the graph. The correlation values of rho were -0.633 for ADC (a) and 0.633 for eADC (b) in Reader 1, while they were -0.528 for ADC (c) and 0.503 for eADC (d) in Reader 2.



our study, the interreader variability was investigated. The mean difference of eADC in PZ cancer and benign tissue was 4% and 7.9%, respectively, and the results were similar with ADC (PZ cancers, 5.8%; benign tissues, 6%).

Our study had several limitations. First, a retrospective study design was used, and we excluded small prostate cancers of $<0.5 \text{ cm}^3$. This may lead to a selection bias such as relatively low proportion of subjects with Gleason Score 6. However, prostate

cancers of $<0.5 \text{ cm}^3$ are considered clinically insignificant.^{21,22} Further studies including small volume of cancers are required to validate our results in natural population with the prostate cancer. Second, visual analyses such as cancer localization or staging were not conducted in our study. These analyses may be a prerequisite to determining whether an imaging technique is clinically useful. Our preliminary quantitative results of eADC might support further qualitative analyses. Third, we did not evaluate the central gland cancers, although approximately 30%

Table 4. Lesion-to-background contrast ratios between apparent diffusion coefficient (ADC) and exponential apparent diffusion coefficient (eADC) maps

Parameter	ADC ($\times 10^{-3} \text{ mm}^2 \text{ s}^{-1}$)	eADC	<i>p</i> -value ^a
Reader 1	2.21 (1.40–4.16)	2.43 (1.44–4.12)	<0.001
Reader 2	2.12 (1.47–4.59)	2.23 (1.46–5.64)	<0.001

Data are the mean values (range).

^aStatistical comparison between ADC and eADC.

of prostate cancers arise from the central gland which consists of a transition zone and central zone.²³ Further study will be needed. Finally, the effect of post-biopsy haemorrhage on the measurement of eADC was not considered. Because the cancer was analysed based on radiological–pathological correlation, we could minimize the adverse effect of post-biopsy haemorrhage.

In conclusion, our preliminary results suggest that the eADC from DWI may have comparable feasibility in discriminating PZ cancers from benign PZ tissues, as compared with ADC. Nevertheless, the eADC may allow improved tissue contrast by higher lesion-to-background ratio. Further prospective studies are needed to validate its clinical utility in prostate cancer.

REFERENCES

- Vargas HA, Akin O, Franiel T, Mazaheri Y, Zheng J, Moskowitz C, et al. Diffusion-weighted endorectal MR imaging at 3 T for prostate cancer: tumor detection and assessment of aggressiveness. *Radiology* 2011; **259**: 775–84. doi: [10.1148/radiol.11102066](https://doi.org/10.1148/radiol.11102066)
- Tan CH, Wang J, Kundra V. Diffusion weighted imaging in prostate cancer. *Eur Radiol* 2011; **21**: 593–603. doi: [10.1007/s00330-010-1960-y](https://doi.org/10.1007/s00330-010-1960-y)
- Wu LM, Xu JR, Ye YQ, Lu Q, Hu JN. The clinical value of diffusion-weighted imaging in combination with T2-weighted imaging in diagnosing prostate carcinoma: a systematic review and meta-analysis. *AJR Am J Roentgenol* 2012; **199**: 103–10. doi: [10.2214/AJR.11.7634](https://doi.org/10.2214/AJR.11.7634)
- Afaq A, Koh DM, Padhani A, van As N, Sohaib SA. Clinical utility of diffusion-weighted magnetic resonance imaging in prostate cancer. *BJU Int* 2011; **108**: 1716–22. doi: [10.1111/j.1464-410X.2011.10256.x](https://doi.org/10.1111/j.1464-410X.2011.10256.x)
- Barentsz JO, Richenberg J, Clements R, Choyke P, Verma S, Villeirs G, et al. ESUR prostate MR guidelines 2012. *Eur Radiol* 2012; **22**: 746–57. doi: [10.1007/s00330-011-2377-y](https://doi.org/10.1007/s00330-011-2377-y)
- Rosenkrantz AB, Kong X, Niver BE, Berkman DS, Melamed J, Babb JS, et al. Prostate cancer: comparison of tumor visibility on trace diffusion-weighted images and the apparent diffusion coefficient map. *AJR Am J Roentgenol* 2011; **196**: 123–9. doi: [10.2214/AJR.10.4738](https://doi.org/10.2214/AJR.10.4738)
- Oto A, Kayhan A, Jiang Y, Tretiakova M, Yang C, Antic T, et al. Prostate cancer: differentiation of central gland cancer from benign prostatic hyperplasia by using diffusion-weighted and dynamic contrast-enhanced MR imaging. *Radiology* 2010; **257**: 715–23. doi: [10.1148/radiol.10100021](https://doi.org/10.1148/radiol.10100021)
- Hambroek T, Somford DM, Huisman HJ, van Oort IM, Witjes JA, Hulsbergen-van de Kaa CA, et al. Relationship between apparent diffusion coefficients at 3.0-T MR imaging and Gleason grade in peripheral zone prostate cancer. *Radiology* 2011; **259**: 453–61. doi: [10.1148/radiol.11091409](https://doi.org/10.1148/radiol.11091409)
- Hambroek T, Hoeks C, Hulsbergen-van de Kaa C, Scheenen T, Futterer J, Bouwense S, et al. Prospective assessment of prostate cancer aggressiveness using 3-T diffusion-weighted magnetic resonance imaging-guided biopsies versus a systematic 10-core transrectal ultrasound prostate biopsy cohort. *Eur Urol* 2012; **61**: 177–84. doi: [10.1016/j.eururo.2011.08.042](https://doi.org/10.1016/j.eururo.2011.08.042)
- Zhang YL, Yu BL, Ren J, Qu K, Wang K, Qiang YQ, et al. EADC values in diagnosis of renal lesions by 3.0 T diffusion-weighted magnetic resonance imaging: compared with the ADC values. *Appl Magn Reson* 2013; **44**: 349–63. doi: [10.1007/s00723-012-0376-z](https://doi.org/10.1007/s00723-012-0376-z)
- Provenzale JM, Engelter ST, Petrella JR, Smith JS, MacFall JR. Use of MR exponential diffusion-weighted images to eradicate T2 “shine-through” effect. *AJR Am J Roentgenol* 1999; **172**: 537–9. doi: [10.2214/ajr.172.2.9930819](https://doi.org/10.2214/ajr.172.2.9930819)
- Engelter ST, Provenzale JM, Petrella JR, Alberts MJ, DeLong DM, MacFall JR. Use of exponential diffusion imaging to determine the age of ischemic infarcts. *J Neuroimaging* 2001; **11**: 141–7. doi: [10.1111/j.1552-6569.2001.tb00024.x](https://doi.org/10.1111/j.1552-6569.2001.tb00024.x)
- Tsang BK, Foster E, Kam A, Storey E. Diffusion weighted imaging with trace diffusion weighted imaging, the apparent diffusion coefficient and exponential images in the diagnosis of spinal cord infarction. *J Clin Neurosci* 2013; **20**: 1630–2. doi: [10.1016/j.jocn.2012.10.011](https://doi.org/10.1016/j.jocn.2012.10.011)
- Dickinson L, Ahmed HU, Allen C, Barentsz JO, Carey B, Futterer JJ, et al. Magnetic resonance imaging for the detection, localisation, and characterisation of prostate cancer: recommendations from a European consensus meeting. *Eur Urol* 2011; **59**: 477–94. doi: [10.1016/j.eururo.2010.12.009](https://doi.org/10.1016/j.eururo.2010.12.009)
- Vargas HA, Akin O, Shukla-Dave A, Zhang J, Zakian KL, Zheng J, et al. Performance characteristics of MR imaging in the evaluation of clinically low-risk prostate cancer: a prospective study. *Radiology* 2012; **265**: 478–87. doi: [10.1148/radiol.12120041](https://doi.org/10.1148/radiol.12120041)
- Simon JE, Czechowsky DK, Hill MD, Harris AD, Buchan AM, Frayne R. Fluid-attenuated inversion recovery preparation: not an improvement over conventional diffusion-weighted imaging at 3T in acute ischemic stroke. *AJNR Am J Neuroradiol* 2004; **25**: 1653–8.
- Olsen OE, Sebire NJ. Apparent diffusion coefficient maps of pediatric mass lesions with free-breathing diffusion-weighted magnetic resonance: feasibility study. *Acta Radiol* 2006; **47**: 198–204. doi: [10.1080/02841850500479651](https://doi.org/10.1080/02841850500479651)
- Heidenreich A, Bastian PJ, Bellmunt J, Bolla M, Joniau S, van der Kwast T, et al. EAU guidelines on prostate cancer. Part 1: screening, diagnosis, and local treatment with curative intent-update 2013. *Eur Urol* 2014; **65**: 124–37. doi: [10.1016/j.eururo.2013.09.046](https://doi.org/10.1016/j.eururo.2013.09.046)
- Verma S, Rajesh A, Morales H, Lemen L, Bills G, Delworth M, et al. Assessment of aggressiveness of prostate cancer: correlation of apparent diffusion coefficient with histologic grade after radical prostatectomy. *AJR Am J Roentgenol* 2011; **196**: 374–81. doi: [10.2214/AJR.10.4441](https://doi.org/10.2214/AJR.10.4441)
- van den Bergh RC, Ahmed HU, Bangma CH, Cooperberg MR, Villers A, Parker CC. Novel tools to improve patient selection and monitoring on active surveillance for low-risk prostate cancer: a systematic review. *Eur Urol* 2014; **65**: 1023–31. doi: [10.1016/j.eururo.2014.01.027](https://doi.org/10.1016/j.eururo.2014.01.027)
- Stamey TA, Freiha FS, McNeal JE, Redwine EA, Whittamore AS, Schmid HP. Localized prostate cancer. Relationship of tumor volume to clinical significance for treatment of prostate cancer. *Cancer* 1993; **71**(Suppl. 3): 933–8. doi: [10.1002/1097-0142\(19930201\)71:3+<933::AID-CNCR2820711408>3.0.CO;2-L](https://doi.org/10.1002/1097-0142(19930201)71:3+<933::AID-CNCR2820711408>3.0.CO;2-L)
- Ochiai A, Troncoso P, Chen ME, Lloreta J, Babaian RJ. The relationship between tumor volume and the number of positive cores in men undergoing multisite extended biopsy: implication for expectant management. *J Urol* 2005; **174**: 2164–8. doi: [10.1097/01.ju.0000181211.49267.43](https://doi.org/10.1097/01.ju.0000181211.49267.43)
- McNeal JE, Redwine EA, Freiha FS, Stamey TA. Zonal distribution of prostatic adenocarcinoma. Correlation with histologic pattern and direction of spread. *Am J Surg Pathol* 1988; **12**: 897–906. doi: [10.1097/0000478-198812000-00001](https://doi.org/10.1097/0000478-198812000-00001)